Available online at www.sciencedirect.com

ScienceDirect

Journal of Sound and Vibration 313 (2008) 367–374

JOURNAL OF SOUND AND VIBRATION

www.elsevier.com/locate/jsvi

Rapid Communication

Existence of super-harmonics in quarter-vehicle system responses with nonlinear inertia hydraulic track mount given sinusoidal force excitation

Jun Hwa Lee, Rajendra Singh*

Acoustics and Dynamics Laboratory, Department of Mechanical Engineering, The Ohio State University, Columbus, OH 43210, USA

Received 11 November 2007; accepted 15 February 2008
Handling Editor: S. Bolton

Abstract

Hydraulic engine mounts (and other elastomeric devices) are usually experimentally characterized based on the assumption that mount response to harmonic displacement input is purely sinusoidal, although they contain strong super-harmonics. Time domain responses of a quarter-vehicle system with a nonlinear inertia track-type mount are examined in this communication, with emphasis on the super-harmonics. Finally, internal (mount) path forces are evaluated in order to clarify their contribution to the system responses and the effect of nonlinearities.

1. Introduction

Mounts are typically characterized by a non-resonant elastomer test in terms of the dynamic transfer stiffness $K(\omega,X) = F_T/X$ at a given angular excitation frequency ω (rad/s) and amplitude X of sinusoidal displacement excitation, under a specific static load f_s (or displacement); here F_T is the amplitude of the force transmitted to a blocked base only at primary ω though super-harmonics might be present [1–5]. Nevertheless, the hydraulic engine mount is truly a nonlinear isolator and as such the upper chamber pressure and transmitted force time histories, when excited by a purely sinusoidal displacement input, are often periodic with super-harmonic (and sub-harmonic) contents [1–5]. Although the nonlinear phenomena of device (alone) have been experimentally and analytically studied [1–14], their effects on the vehicle system response are still poorly understood to the best of our knowledge. For instance, several investigators, including Kim and Singh [2], and Royston and Singh [3], have developed nonlinear time domain models of the mount but the thrust of prior work has been the fundamental harmonic and comparison with measured $K(\omega,X)$ in frequency domain. To demonstrate the existence of super-harmonics, we have initiated an improved nonlinear analysis and in particular this communication presents a first report on the effect of inertia track-type mount on the dynamic behavior of a quarter vehicle (as shown in Fig. 1). We will employ the measured time domain data (from our

*Corresponding author. Tel.: +1 614 292 9044; fax: +1 614 292 3163.
E-mail address: singh.3@osu.edu (R. Singh).

0022-460X/$ - see front matter
doi:10.1016/j.jsv.2008.02.025

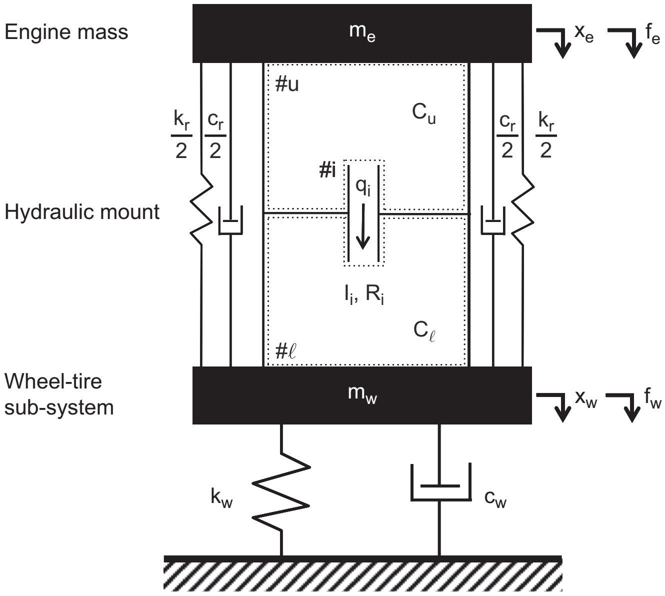

Fig. 1. Quarter-vehicle system with nonlinear hydraulic (inertia track-type) engine mount.

laboratory [4–5]) on mount alone and then we predict the response of the system (of Fig. 1) in time domain including the super-harmonics. Two dominant nonlinearities of this mount are: (i) dual-staged compliance of the upper chamber that includes the vacuum formation during the expansion process [1–6] and (ii) nonlinear fluid resistance of the inertia track [1–5]. We will also compare the relative contributions of detailed force paths such as rubber and fluid paths in the mount, as a function of ω, to clarify their roles from the system viewpoint.

2. Nonlinearities of inertia track-type mount

2.1. Super-harmonic contents in measured signals for mount alone

Fig. 2 shows the measured harmonic responses of a hydraulic engine mount with inertia track only (as shown in Fig. 1) when excited by the conventional sinusoidal displacement input. Observe the flattened region in the upper chamber pressure $p_u(t)$ in Fig. 2(a); this shape suggests that the vacuum conditions exist in the upper chamber [1–6]. However, the shapes of $p_u(t)$ in Figs. 2(a) and (b) are qualitatively different, though both represent the harmonic responses of the same mount. The vacuum phenomenon is less prominent in Fig. 2(b), due to lower negative $p_u(t)$. Table 1 shows the measured super-harmonics where the ratios (in %) of nth Fourier coefficient (Φ_n) to the fundamental harmonic ($n = 1$) are listed. The second harmonic is significantly higher when $p_u(t)$ has a flattened shape; otherwise the third harmonic is dominant.

2.2. Physics of the nonlinear phenomena

The nonlinear fluid model of the mount (Fig. 1) is briefly examined to clarify the source(s) of super-harmonic contents. In order to focus on the inertia track mount only, assume that the masses m_e and m_w of Fig. 1 are zero and infinity, respectively; and, the stiffness k_w and damping coefficient c_w are zero. In addition, designate the displacement x_e and force f_e as x and f (for the sake of convenience) when the mount alone is considered. For the fluid model of Fig. 1, the rubber path is given by stiffness k_r and damping c_r coefficients; $C_u(p_u)$ and C_l are the fluid compliances of the upper (#u) and lower (#ℓ) chambers; $q_i(t)$ is the volumetric flow rate through the inertia track (#i); I_i is the inertia of fluid column in the track; and $R_i(q_i)$ is the fluid resistance of the track. The dynamic component of driving point force $f(t)$ is expressed as follows where $x(t)$ is the

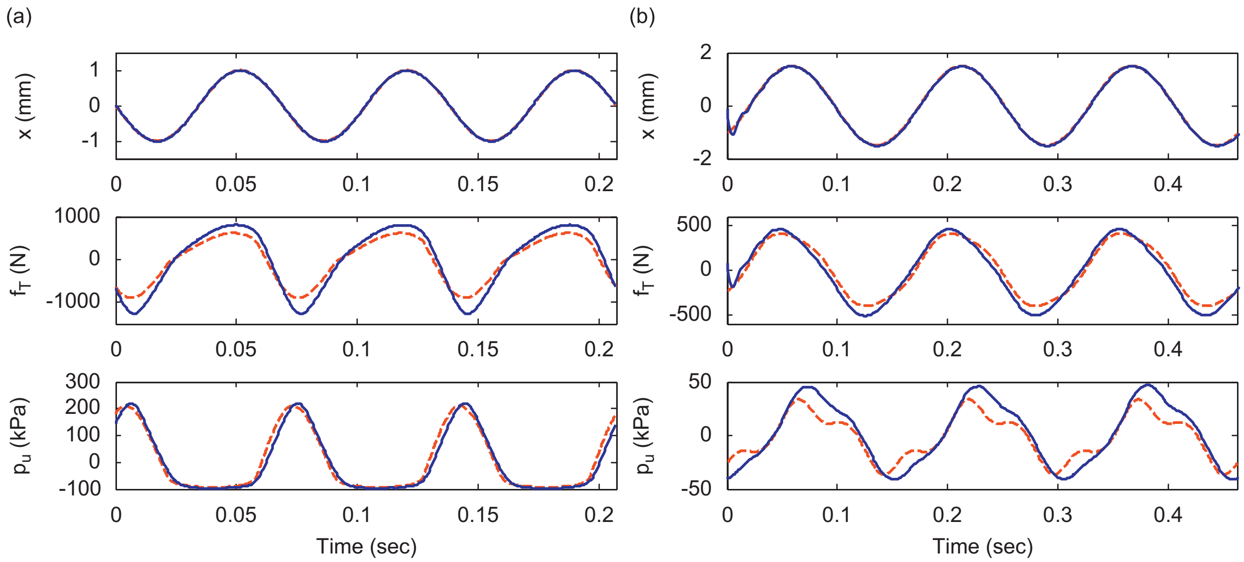

Fig. 2. Time domain responses of the hydraulic (inertia track) mount when excited by harmonic displacement: (a) displacement x at 14.5 Hz with $X = 1$ mm, transmitted force f_T and upper chamber pressure p_u, (b) x (at 6.5 Hz with $X = 1.5$ mm), f_T and p_u. Key: ___, measured; _ _ _ _, predicted.

Table 1
Measured and predicted super-harmonics in steady-state time domain responses of the mount (alone)

Fourier coefficient (Φ_n) ratio (%)	$\lvert\Phi_2\rvert/\lvert\Phi_1\rvert$	$\lvert\Phi_3\rvert/\lvert\Phi_1\rvert$	$\lvert\Phi_4\rvert/\lvert\Phi_1\rvert$	$\lvert\Phi_5\rvert/\lvert\Phi_1\rvert$
Harmonic excitation at 14.5 Hz with $X = 1$ mm (measured)				
f_T	28.7	5.70	0.46	0.87
p_u	41.6	7.80	0.72	1.29
Harmonic excitation at 14.5 Hz with $X = 1$ mm (predicted)				
f_T	27.1	3.02	3.49	0.57
p_u	40.2	4.47	5.17	0.84
Harmonic excitation at 6.5 Hz with $X = 1.5$ mm (measured)				
f_T	1.87	5.14	0.43	0.81
p_u	2.22	13.5	1.01	0.91
Harmonic excitation at 6.5 Hz with $X = 1.5$ mm (predicted)				
f_T	0.01	7.40	0.02	0.48
p_u	0.06	33.3	0.09	2.14

dynamic displacement; A_p is the effective rubber (piston) area; $p_u(t)$ and $p_\ell(t)$ are the dynamic pressures of the upper and lower chambers:

$$f(t) = c_r\dot{x}(t) + k_r x(t) - A_p p_u(t). \tag{1}$$

Nonlinear and linear continuity equations for the upper and lower chambers are written as follows:

$$q_i(t) - C_u(p_u)\dot{p}_u(t) = A_p\dot{x}(t), \quad q_i(t) + C_\ell\dot{p}_\ell(t) = 0. \tag{2,3}$$

Nonlinear momentum equation for the inertia track is

$$I_i\dot{q}_i(t) + R_i(q_i)q_i(t) + p_u(t) - p_\ell(t) = 0. \tag{4}$$

The dynamic component of the force $f_T(t)$ transmitted to the rigid base (when m_w is ∞) is related to $f(t)$ as follows:

$$f_T(t) = c_r\dot{x}(t) + k_r x(t) - A_p p_u(t) = f(t). \tag{5}$$

Parameters and empirical functions [4,5] of the example case (inertia track mount) are as follows: Nonlinear $C_u(p_u)$ is $2.5\times10^{-11}\,\mathrm{m^5\,N^{-1}}$ when $p_u \geqslant 0$ but 2.5×10^{-11}–$7\times10^{-45}p_u{}^7\,\mathrm{m^5\,N^{-1}}$ when $p_u < 0$ (where p_u is in Pa); C_ℓ is $2.4\times10^{-9}\,\mathrm{m^5\,N^{-1}}$; A_p is $3.31\times10^{-3}\,\mathrm{m^2}$; I_i is $2.8\times10^{6}\,\mathrm{kg\,m^{-4}}$; nonlinear $R_i(q_i)$ is $3.45\times10^{11}|q_i|\,\mathrm{N\,s\,m^{-5}}$ (where q_i is in $\mathrm{m^3\,s^{-1}}$); k_r and c_r are $3.2\times10^{5}\,\mathrm{N\,m^{-1}}$ and $5.0\times10^{2}\,\mathrm{N\,s\,m^{-1}}$. With the above-mentioned nonlinear parameters, $C_u(p_u)$ and $R_i(q_i)$, the governing equations (1)–(5) are simulated. Predicted time histories (dotted lines) in Fig. 2 illustrate that Eqs. (1)–(5) faithfully represent the measured nonlinear phenomena. Table 1 confirms that the nonlinear fluid model reproduces the largest super-harmonic content in two cases. When p_u experiences severe vacuum condition, second harmonic is strong; this suggests that the nonlinearity associated with $C_u(p_u)$ is more dominant. Note that the $R_i(q_i)$ nonlinearity by itself can produce only odd super-harmonics and thus strong third harmonic is found when vacuum condition is insignificant. Accordingly, $R_i(q_i)$ is a more dominant nonlinearity in this case.

3. Responses of the quarter-vehicle system with nonlinear mount

3.1. Frequency domain responses

Consider a simplified engine-mount–wheel-tire system as shown in Fig. 1. For the sake of illustration, assume that the engine mass m_e is 120 kg and the wheel-axle mass m_w is 40 kg; the tire stiffness k_w and damping coefficient c_w are $2\times10^{5}\,\mathrm{N\,m^{-1}}$ and $500\,\mathrm{N\,s\,m^{-1}}$. The governing equations consist of the following expressions along with Eqs. (3) and (4) where x_e and x_w are the displacements of the engine and wheel axle; and f_e and f_w are the external forces applied to masses m_e and m_w, respectively:

$$m_e\ddot{x}_e + c_r(\dot{x}_e - \dot{x}_w) + k_r(x_e - x_w) - A_p p_u = f_e, \tag{6}$$

$$m_w\ddot{x}_w + c_w\dot{x}_w + k_w x_w + c_r(\dot{x}_w - \dot{x}_e) + k_r(x_w - x_e) + A_p p_u = f_w, \tag{7}$$

$$q_i - C_u(p_u)\dot{p}_u = A_p(\dot{x}_e - \dot{x}_w). \tag{8}$$

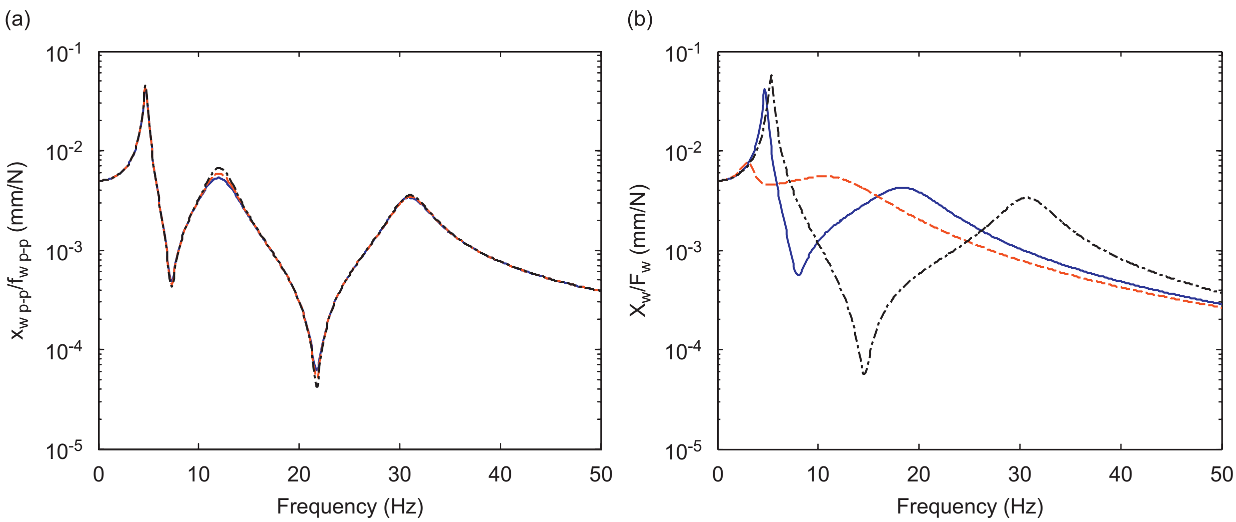

Fig. 3. Effect of the force excitation level on frequency domain responses of the system with nonlinear mount: (a) normalized frequency response x_{wp-p}/f_{wp-p} of the nonlinear system. Key: ___, $f_{wp-p} = 130$ N; _ _ _ _, $f_{wp-p} = 97.5$ N; _ . _, $f_{wp-p} = 65$ N; in all cases $f_{ep-p} = 0$ N. (b) Corresponding frequency response functions X_w/F_w of three equivalent linear systems. Key: ____, linearized at first resonant frequency; _ _ _ _, linearized at second resonant frequency; _ . _, linearized at third resonant frequency.

Note that Eqs. (4) and (8) are nonlinear differential equations. Fig. 3(a) shows the normalized frequency responses in terms of x_{wp-p}/f_{wp-p} of the quarter-vehicle system under harmonic force excitation $f_w = F_w \sin \omega t$ (but $f_e = 0$). The system is apparently a two-degree-of-freedom system but an additional degree of freedom is brought in by the mount's inertia track dynamics. Observe that the nonlinear frequency responses are excitation amplitude-sensitive while each curve looks like a frequency response function of a linear time-invariant (LTI) three-degree-of-freedom system. The resonant frequencies are nearly identical, which means that only damping (at the resonances) is affected by the excitation amplitude. Fig. 3(b) illustrates the frequency response functions of the equivalent LTI systems at three resonant frequencies. Parameters of the equivalent Kelvin–Voigt model (stiffness k_e and damping coefficient c_e) for the inertia track mount are determined from the complex stiffness $\Phi_1(f_H)/\Phi_1(x_e - x_w)$ by exciting the system at each resonant frequency. Here f_H is the internal (total) force generated by the inertia track mount: $f_H = c_r(\dot{x}_e - \dot{x}_w) + k_r(x_e - x_w) - A_p p_u$. The behavior of the equivalent linear system with light damping is similar to that of the nonlinear system near the associated resonant frequency. Accordingly, the linearization technique works for two lightly damped (first and third) modes but not for the heavily damped second mode.

3.2. Super-harmonics in time domain responses under resonant excitations

Fig. 4 shows the steady-state time domain responses of the system given harmonic force excitation with $f_{wp-p} = 130$ N (and $f_{ep-p} = 0$ N) at the resonant frequencies. Table 2 shows the super-harmonic contents.

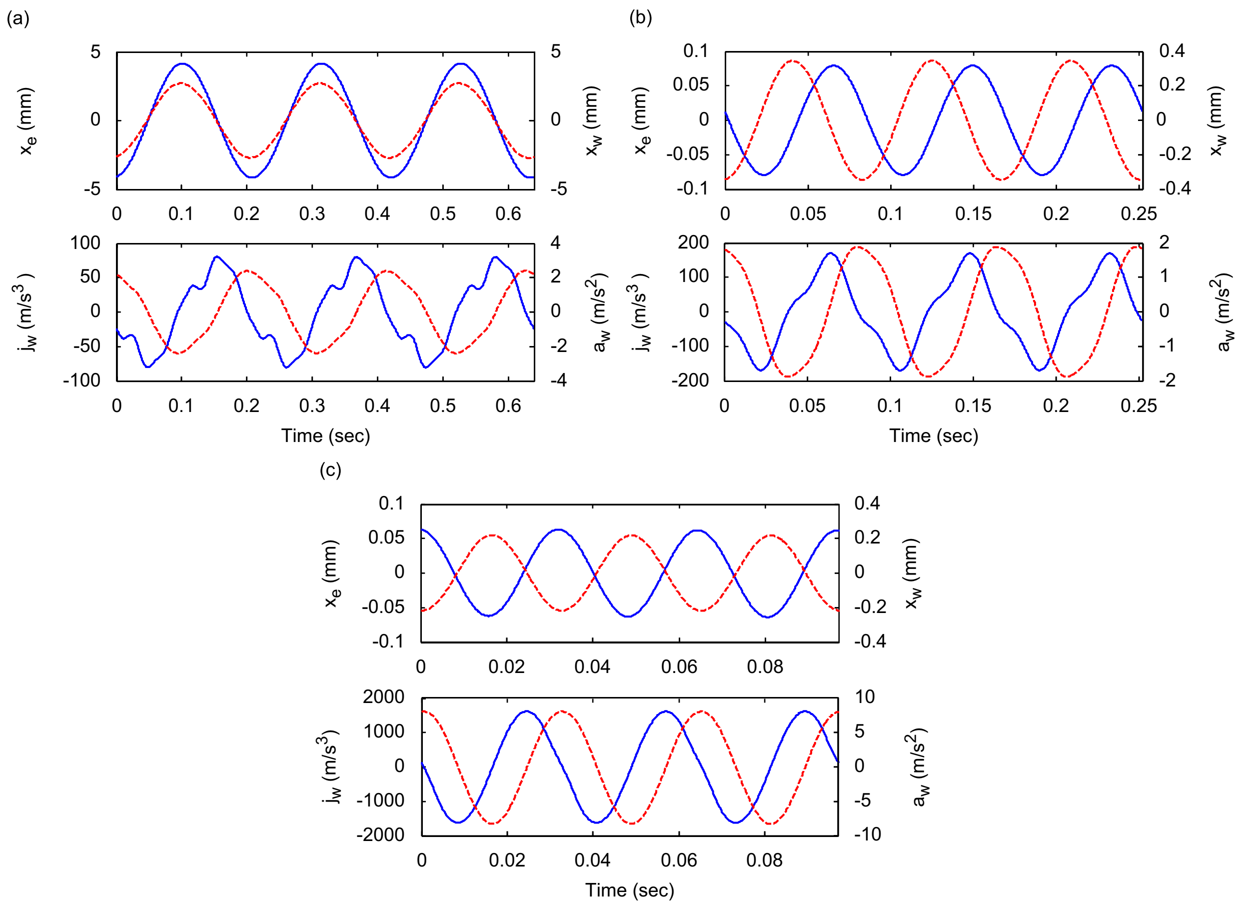

Fig. 4. Steady-state time domain responses of the system when excited by the harmonic force $f_{wp-p} = 130$ N (and $f_{ep-p} = 0$ N): (a) displacements x_e and x_w, jerk j_w, and acceleration a_w when excited at the first resonance, (b) x_e, x_w, j_w, and a_w when excited at the second resonance, (c) x_e, x_w, j_w, and a_w when excited at the third resonance. Key: ____, x_e, j_w; _ _ _ _, x_w, a_w.

Table 2
Super-harmonics in steady-state time domain responses of the system when excited by harmonic force $f_{wp-p} = 130\,\mathrm{N}$ (and $f_{ep-p} = 0\,\mathrm{N}$) at three resonances

Fourier coefficient (Φ_n) ratio (%)	$\lvert\Phi_2\rvert/\lvert\Phi_1\rvert$	$\lvert\Phi_3\rvert/\lvert\Phi_1\rvert$	$\lvert\Phi_4\rvert/\lvert\Phi_1\rvert$	$\lvert\Phi_5\rvert/\lvert\Phi_1\rvert$	Effect of harmonic order n
Harmonic excitation at first resonant frequency (4.7 Hz)					
f_H	0.00	0.54	0.00	0.25	
p_u	0.00	12.3	0.00	1.25	
x_w	0.00	0.71	0.00	0.06	$1/n^2$
v_w	0.00	2.14	0.00	0.30	$1/n$
a_w	0.00	6.42	0.00	1.51	1
j_w	0.00	19.3	0.00	7.54	n
Harmonic excitation at second resonant frequency (11.9 Hz)					
f_H	0.07	8.54	0.05	0.17	
p_u	0.02	3.46	0.02	0.08	
x_w	0.02	0.72	0.00	0.00	$1/n^2$
v_w	0.03	2.17	0.01	0.02	$1/n$
a_w	0.06	6.50	0.03	0.12	1
j_w	0.13	19.5	0.14	0.62	n
Harmonic excitation at third resonant frequency (30.9 Hz)					
f_H	1.27	0.75	0.42	0.19	
p_u	1.74	1.07	0.61	0.28	
x_w	0.28	0.08	0.03	0.01	$1/n^2$
v_w	0.57	0.22	0.09	0.03	$1/n$
a_w	1.13	0.65	0.37	0.17	1
j_w	2.26	1.96	1.47	0.84	n

The third harmonic is dominant when the system is excited at the first (4.7 Hz) and second (11.9 Hz) resonant frequencies. The upper chamber does not undergo severe vacuum and hence $R_i(q_i)$ governs the nonlinear dynamics of the underlying system at these two modes. However, the second harmonic is the largest when excited at the third resonant frequency (30.9 Hz). This suggests that the primary nonlinear source now is the vacuum phenomenon. But its contribution is not significant as the flattened region in p_u is not prominent due to smaller relative displacement response. Note that x_e and x_w look like pure sinusoids, although the net constraint forces f_e–f_H and $f_w + f_H - k_w x_w - c_w \dot{x}_w$ contain super-harmonics. The nth harmonic in the mount force affects the displacement x_w, velocity $v_w(= \dot{x}_w)$, acceleration $a_w(= \ddot{x}_w)$, and jerk $j_w(= \dddot{x}_w)$ with the ratios of $1/n^2$, $1/n$, 1, and n respectively, as shown in Table 2, where n is the harmonic order. Accordingly, super-harmonics (due to mount nonlinearities) should be more evident in system acceleration or jerk signatures.

Fig. 4 also shows the mode shapes of the system from the time domain responses. At the first resonance (wheel hop mode), x_e and x_w are nearly in-phase with each other: $\Phi_1(x_e) = 4.1\angle -171.7^\circ$ and $\Phi_1(x_w) = 2.7\angle -168.5^\circ$. At the second resonance (engine bounce mode), phase of x_e is nearly 90° with respect to x_w: $\Phi_1(x_e) = 7.9 \times 10^{-2}\angle 80.0^\circ$ and $\Phi_1(x_w) = 3.5 \times 10^{-1}\angle -176.6^\circ$. Observe that the engine bounce mode is heavily damped due to significant damping introduced by the inertia track. At the third resonance (inertia track mode), m_e and m_w move nearly 180° out-of-phase with each other: $\Phi_1(x_e) = 6.3 \times 10^{-2}\angle 4.2^\circ$ and $\Phi_1(x_w) = 2.2 \times 10^{-1}\angle 175.6^\circ$. The first and third mode shapes with light damping can also be obtained by employing the equivalent Kelvin–Voigt model and by solving the conventional eigenvalue problem. For instance, the eigenvectors $\{u_e \quad u_w\}^{\mathrm{T}}$ are obtained by using the three equivalent linear systems (Fig. 3(b)) as follows: $\{11.1\angle -45.1^\circ \quad 7.1\angle -44.5^\circ\}^{\mathrm{T}}$, $\{2.4\angle 1.0^\circ \quad 12.8\angle 133.1^\circ\}^{\mathrm{T}}$, and $\{2.1\angle 132.7^\circ \quad 7.2\angle -44.4^\circ\}^{\mathrm{T}}$. At the first and third modes, we obtain nearly identical eigenvectors but not at the second mode.

4. Contribution of rubber and fluid paths (within the mount) from the system perspective

Consider the fluid model of mount as shown in Fig. 1 again. The total (internal) force f_H consists of the force through the rubber path $f_r(=c_r(\dot{x}_e-\dot{x}_w)+k_r(x_e-x_w))$ and the force through the fluid path $f_f(=-A_p p_u)$. Fig. 5(a) shows the internal force spectra. The rubber path force interferes with the fluid path force in a destructive manner when the excitation frequency is less than the frequency at which the ratio f_{fp-p}/f_{rp-p} peaks. But they interfere in a constructive fashion beyond this peak frequency. The contribution of the fluid path is most significant near the minimum of the rubber path force. Since $c_r(\dot{x}_e-\dot{x}_w)$ is negligible, $f_r \approx k_r(x_e-x_w)$. Accordingly, the fluid path dominates near the anti-resonance of the relative displacement $x_e - x_w$ when excited by the harmonic force. The fluid path force f_f can be rewritten using Eqs. (3) and (4) as

$$f_f = A_p\left(I_i\dot{q}_i + R_i(q_i)q_i + \frac{1}{C_\ell}\int q_i\,\mathrm{d}t\right). \tag{9}$$

Now it is decomposed into the track inertia force $f_{fI}(=A_pI_i\dot{q}_i)$, the track resistance force $f_{fR}(=A_pR_i(q_i)q_i)$, and the lower chamber compliance force $f_{fC}(=A_p\int q_i\,\mathrm{d}t/C_\ell)$. Fig. 5(b) shows their spectra. Overall, f_{fI} is the dominant component and it is larger than f_{fR} even at the first and second resonances of the system. Although the quadratic nonlinearity of $R_i(q_i)$ is the primary source of the third harmonic, the most significant component is still f_{fI}. This suggests that the nonlinear $R_i(q_i)$ affects the system behavior in an indirect manner.

5. Conclusion

The nonlinear upper chamber compliance and fluid resistance of the hydraulic (inertia track) mount were evaluated from the vehicle system perspective. Although the vacuum phenomenon is very prominent in mount (alone) tests, its effect on the system responses is insignificant due to small relative displacement response. System acceleration and jerk responses show strong super-harmonics that are introduced by the mount. While the fluid resistance is one of the main nonlinear sources, the fluid inertial force (linear term) affects the total (fluid) path force more. Further work on the free decoupler-type mount is in progress and will be reported soon.

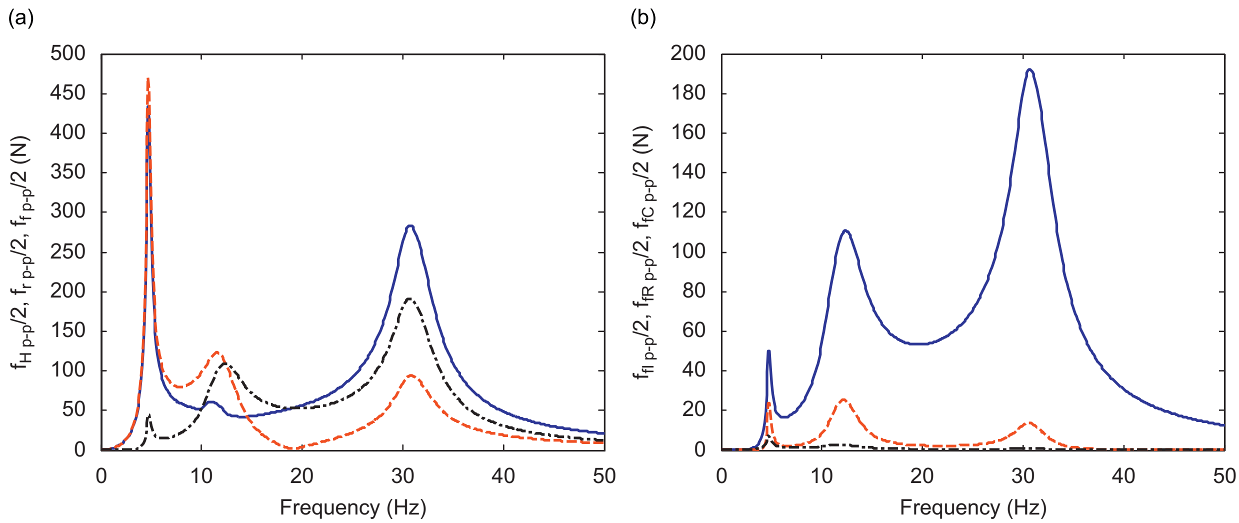

Fig. 5. Spectra of path forces within the system: (a) rubber f_r, fluid f_f and combined f_H path forces. Key: ____, $f_{Hp-p}/2$; _ _ _ _, $f_{rp-p}/2$; _ . _, $f_{fp-p}/2$. (b) Contribution of track inertia f_{fI}, track resistance f_{fR}, and lower chamber compliance f_{fC} path forces. Key: ____, $f_{fIp-p}/2$; _ _ _ _, $f_{fRp-p}/2$; _ . _, $f_{fCp-p}/2$.

Acknowledgments

This work was supported by the Korea Research Foundation Grant (KRF-2006-352-D00035) funded by the Korean Government (MOEHRD).

References

[1] G. Kim, R. Singh, Nonlinear analysis of automotive hydraulic engine mount, *ASME Journal of Dynamic Systems, Measurement and Control* 115 (1993) 482–487.

[2] G. Kim, R. Singh, A study of passive and adaptive hydraulic engine mount systems with emphasis on non-linear characteristics, *Journal of Sound and Vibration* 179 (3) (1995) 427–453.

[3] T.J. Royston, R. Singh, Vibratory power flow through a non-linear path into a resonant receiver, *Journal of the Acoustical Society of America* 101 (4) (1997) 2059–2069.

[4] H. Adiguna, M. Tiwari, R. Singh, H.E. Tseng, D. Hrovat, Transient response of a hydraulic engine mount, *Journal of Sound and Vibration* 268 (2003) 217–248.

[5] M. Tiwari, H. Adiguna, R. Singh, Experimental characterization of a nonlinear hydraulic engine mount, *Noise Control Engineering Journal* 51 (1) (2003) 36–49.

[6] S. He, R. Singh, Discontinuous compliance nonlinearities in the hydraulic engine mount, *Journal of Sound and Vibration* 307 (2007) 545–563.

[7] A.K.W. Ahmed, M.M. Haque, S. Rakhejia, Nonlinear analysis of automotive hydraulic mounts for isolation of vibration and shock, *International Journal of Vehicle Design* 22 (1999) 116–128.

[8] M.F. Golnaraghi, G.N. Jazar, Development and analysis of a simplified nonlinear model of a hydraulic engine mount, *Journal of Vibration and Control* 7 (2001) 495–526.

[9] A. Geisberger, A. Khajepour, F. Golnaraghi, Non-linear modeling of hydraulic mounts: theory and experiment, *Journal of Sound and Vibration* 249 (2) (2002) 371–397.

[10] G.N. Jazar, M.F. Golnaraghi, Nonlinear modeling, experimental verification, and theoretical analysis of a hydraulic engine mount, *Journal of Vibration and Control* 8 (2002) 87–116.

[11] M.S. Foumani, A. Khajepour, M. Durali, Application of sensitivity analysis to the development of high performance adaptive hydraulic engine mounts, *Vehicle System Dynamics* 39 (4) (2003) 257–278.

[12] J.-H. Lee, K.-J. Kim, An efficient technique for design of hydraulic engine mount via design variable-embedded damping modeling, *Journal of Vibration and Acoustics* 127 (2005) 93–99.

[13] J. Christopherson, G.N. Jazar, Dynamic behavior comparison of passive hydraulic engine mounts. Part 1: Mathematical analysis, *Journal of Sound and Vibration* 290 (2006) 1040–1070.

[14] W.-B. Shangguan, Z.-H. Lu, Modelling of a hydraulic engine mount with fluid-structure interaction finite element analysis, *Journal of Sound and Vibration* 275 (2004) 193–221.